High-Performance Epoxy Nanocomposites Reinforced with Three-Dimensional Carbon Nanotube Sponge for Electromagnetic Interference Shielding

Yu Chen, Hao-Bin Zhang, Yanbing Yang, Mu Wang, Anyuan Cao,* and Zhong-Zhen Yu**

Light-weight and high-performance electromagnetic interference (EMI)-shielding epoxy nanocomposites are prepared by an infiltration method using a 3D carbon nanotube (CNT) sponge as the 3D reinforcement and conducting framework. The preformed, highly porous, and electrically conducting framework acts as a highway for electron transport and can resist a high external loading to protect the epoxy nanocomposite. Consequently, a remarkable conductivity of 148 S m^{-1} and an outstanding EMI shielding effectiveness of around 33 dB in the X-band are achieved for the epoxy nanocomposite with 0.66 wt% of CNT sponge, which is higher than that achieved for epoxy nanocomposites with 20 wt% of conventional CNTs. More importantly, the CNT sponge provides a dual advantage over conventional CNTs in its prominent reinforcement and toughening of the epoxy composite. Only 0.66 wt% of CNT sponge significantly increases the flexural and tensile strengths by 102% and 64%, respectively, as compared to those of neat epoxy. Moreover, the nanocomposite shows a 250% increase in tensile toughness and a 97% increase in elongation at break. These results indicate that CNT sponge is an ideal functional component for mechanically strong and high-performance EMI-shielding nanocomposites.

1. Introduction

Currently, electromagnetic interference (EMI) and radiation emitted from electrical equipment and devices are ubiquitous sources of severe pollution, which could severely affect the normal functioning of electronics and the health of human beings. Thus, various EMI-shielding materials have been developed to eliminate unwanted electromagnetic radiation.[1] Recently, light-weight and high-performance polymer composites containing carbon materials have attracted intensive attention because of their unique advantages over conventional, metal, EMI-shielding materials.[2] One- or two-dimensional carbon nanofillers, including carbon nanotubes (CNTs) and graphene sheets, have been used to form electrically conducting networks in polymer matrices.[3]

Nevertheless, high loadings of carbon nanofillers are usually required to get target EMI-shielding effectiveness (SE),[1i,3i,4] which inevitably causes serious processing difficulties and makes the nanocomposites brittle. Elaborate manipulation of the distribution of the filler in the polymer matrix by forming segregated structures or a preferred orientation can improve the EMI-shielding performance and decrease the filler loading.[3j,5] Even so, it is still rather challenging to balance an excellent EMI-shielding performance with optimal mechanical properties of the polymer nanocomposites. Nanofillers usually provide optimal reinforcement to polymers only at low loadings, and a further increase in the loading of these carbon nanofillers often impairs the reinforcement due to the worsened dispersion.[6] Recently, preformed, 3D, interconnected carbon frameworks have been reported for the preparation of functional polymer nanocomposites. Cheng et al.[7] fabricated a lightweight and electrically conductive polydimethylsiloxane (PDMS)/graphene foam composite with excellent EMI-shielding properties. Kim et al.[8] have reported the synthesis of a graphene foam/epoxy composite with a remarkable electrical conductivity of 300 S m^{-1} at 0.2 wt% of graphene foam. It should be noted that in the latter case the nickel foam that was used as a template to synthesize the graphene foam had to be removed using a tedious chemical etching process, and the voids formed after the removal of the nickel template may affect the mechanical properties of the resultant materials.[5,7–9]

Similar to graphene foams, a 3D CNT sponge was also prepared by chemical vapor deposition (CVD) and its applications were explored.[10] Due to its unique architecture and excellent

Dr. Y. Chen, Prof. H.-B. Zhang, M. Wang, Prof. Z.-Z. Yu
State Key Laboratory of Organic-Inorganic Composites
College of Materials Science and Engineering
Beijing University of Chemical Technology
Beijing 100029, P. R. China
E-mail: zhanghaobin@mail.buct.edu.cn;
yuzz@mail.buct.edu.cn
Dr. Y. Yang, Prof. A. Cao
Department of Advanced Materials and Nanotechnology
College of Engineering
Peking University
Beijing 100871, P. R. China
E-mail: anyuan@pku.edu.cn

DOI: 10.1002/adfm.201503782

intrinsic properties, CNT sponges are promising materials to endow polymers with both remarkable reinforcement and EMI-shielding performances. Their template-free synthesis also simplifies the preparation processes of their polymer nanocomposites. Herein, light-weight and high-performance epoxy nanocomposites were prepared by impregnating epoxy into preformed and highly porous 3D CNT sponges. The preformed uniform architecture provided the epoxy with excellent electrical conductivity, EMI-shielding efficiency, and mechanical properties. A remarkable conductivity of 148 S m^{-1} and an outstanding EMI SE of around 33 dB in the X-band were achieved for the epoxy nanocomposite at a low sponge content of 0.66 wt%, which is among the best results for polymer nanocomposites filled with carbon nanofillers.[7,8] Interestingly, the CNT sponge greatly improved both the strength and toughness of the epoxy. The presence of only 0.66 wt% of CNT sponge led to 102% and 64% increases in flexural and tensile strengths, respectively. Furthermore, compared to neat epoxy, the same nanocomposite exhibited a 250% increase in tensile toughness and a 97% increase in elongation at break. The reinforcement and toughening mechanisms are also discussed.

2. Results and Discussion

The microstructure of the CNT sponge was observed using scanning electron microscopy (SEM) and transmission electron microscopy (TEM) (**Figure 1**a,b and Figure S1, Supporting Information). Both techniques showed a highly porous 3D macroscopic structure consisting of randomly distributed multiwalled carbon nanotubes (MWNTs). The intertwined and interconnected CNTs in the sponge hereby act as highways for electron transport and struts to resist external loading, implying their potential in improving the electrical and mechanical properties of epoxy.[11] Note that the CNT sponge exhibits a structure that is formed by physical connections and entanglement with small gaps between the nanotubes, as opposed to the seamless and continuous nanostructures of graphene foams.[7–9,11] In contrast, conventional CNTs with similar diameters generally stack together and suffer from severe agglomeration even after ultrasonic treatment (Figure S2a,b in the Supporting Information).

Epoxy nanocomposites with different contents were prepared by impregnating the epoxy monomer into a highly porous 3D nanostructure with different densities followed by curing. As no solvent was used in the infiltration process, possible voids derived from solvent evaporation could be avoided. As seen in Figure 1c,d, the CNTs were uniformly distributed in the epoxy matrix as individual nanotubes, and the intertwined nanotubes acted as effective junctions to transfer both electrons and external loading. This unique 3D structure made it possible to form interconnected networks in an epoxy matrix even at the low loading of 0.66 wt%. For conventional CNTs, however, similar or higher loadings only led to several CNT-rich zones in the matrix but not to a continuous and interconnected CNT network (Figure S2c,d in the Supporting Information). Because surface modification is usually required to improve the dispersion of conventional CNTs in polymer matrices, this inevitably disrupts their intrinsic surface structure and thus their conductivity. However, the preformed 3D nanostructure of the sponge completely avoids the dispersion problem of the CNTs whereas maintaining its intrinsic surface properties and thus using this

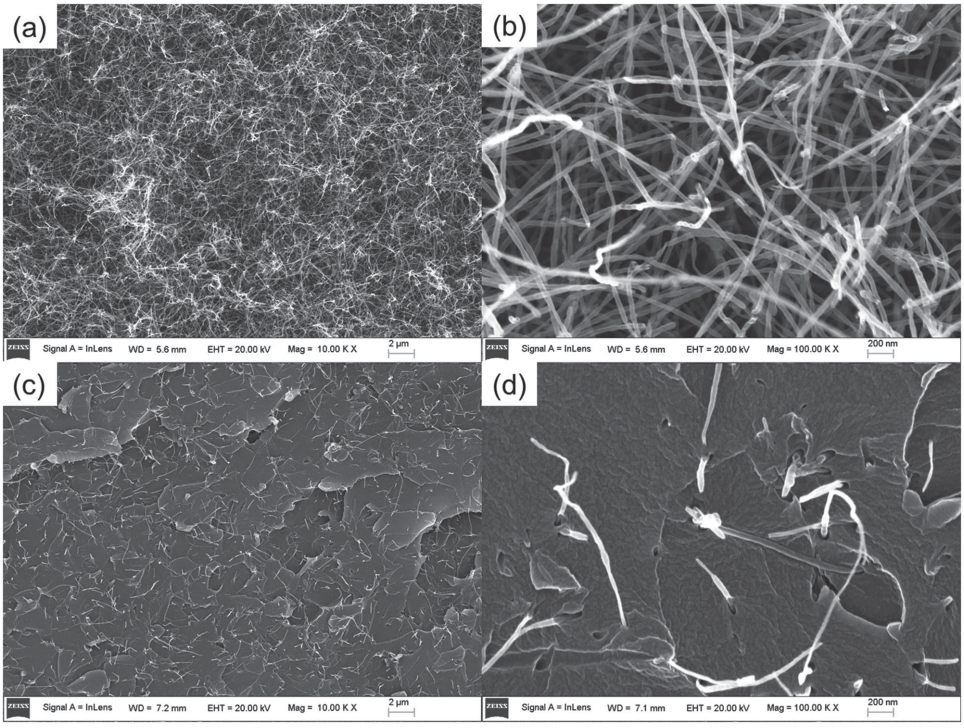

Figure 1. SEM images of a,b) a CNT sponge and c,d) its epoxy nanocomposite at different magnifications.

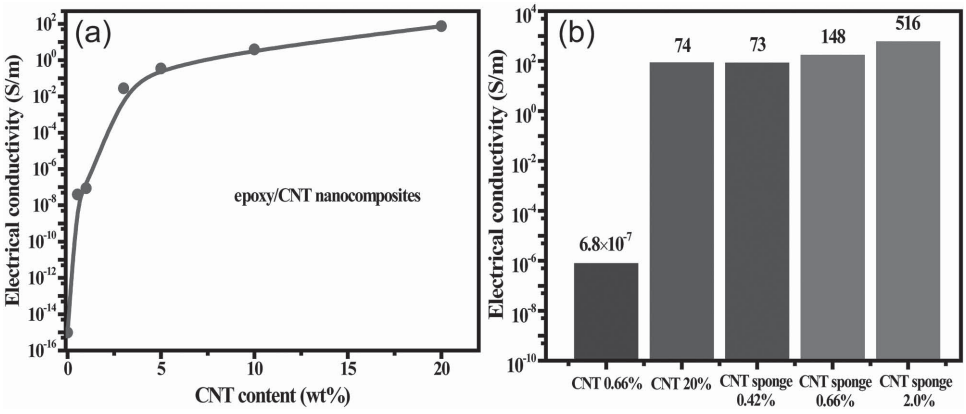

Figure 2. a) Plot of electrical conductivity of epoxy/CNT nanocomposites as a function of CNT content; b) comparison of electrical conductivities of epoxy/CNT sponge and epoxy/CNT nanocomposites.

sponge structure unveils high potential for endowing epoxy structures with a high conductance.[8],[10f]

To identify the superiority of the preformed 3D network, the epoxy/CNT sponge and epoxy/CNT nanocomposites were compared in terms of electrical conductivity (**Figure 2**). As shown in Figure 2a, the epoxy/CNT nanocomposite shows a low electrical conductivity of 6.8×10^{-7} S m^{-1} when a loading of 0.66 wt% of separated CNTs is used, which is consistent with reported values for polymer/CNT nanocomposites.[4a,12] The conductivity increases with increasing CNT content but levels off when the CNT content reaches 3 wt%. Further increasing the content of the CNTs leads to only a limited increment in the electrical conductivity. For example, a conductivity of only 74 S m^{-1} was obtained with 20 wt% of CNTs. On the contrary, a comparable conductivity (73 S m^{-1}) was obtained with only 0.42 wt% CNT content in the epoxy/CNT sponge composite (Figure 2b). Much higher values of 148 and 516 S m^{-1} were achieved with 0.66 and 2.0 wt% of CNT content, respectively, indicating that the favorable 3D conducting framework of the CNT sponge survived during the compounding with the epoxy and curing processes. Therefore, the 3D CNT sponge provides a far superior conductivity as compared to that of conventional CNT/polymer nanocomposites, see **Table 1**.[1h,1i,2a,3b,3i,3j,4a,4b,5,7,12–20]

Previously, an electrical conductivity of 20 S m^{-1} for a CNT/polymer composite was reported but this involved a content of 15 wt% single walled carbon nanotubes (SWNTs)[4a] or 4.23 vol% thermally reduced graphene oxide (TGO).[1i] Li et al.[5] reported a superior EMI SE of 45.1 dB for a polystyrene (PS) nanocomposite with 3.47 vol% reduced graphene oxide (RGO) loading. Kim et al.[21] obtained a conductivity of 20 S m^{-1} for an epoxy nanocomposite with 1.4 wt% RGO by constructing a 3D graphene aerogel. CVD-derived 3D graphene foams have also provided higher conductivities, such as 200 S m^{-1} at 0.8 wt% of graphene foam for a flexible PDMS[7] and 300 S m^{-1} at 0.2 wt% graphene foam for an epoxy foam nanocomposite,[8] which are similar to our results obtained for the epoxy/CNT sponge nanocomposites. It is a valuable achievement to obtain highly conductive epoxy nanocomposites with such a small amount of physically interconnected CNT sponge. Moreover, the template-free synthesis process of the CNT sponge further adds superiority to these polymer nanocomposites as their preparation procedure is much simpler as compared to the template-directed synthesis routine of graphene foams.[7,8] Our epoxy/CNT sponge nanocomposite thus exhibits a high electrical conductivity even when compared to the best values for polymer nanocomposites (Table 1).

To clearly explain the different electrical conductivities, we proposed a schematic that compares the microstructures of the epoxy/CNT and epoxy/CNT sponge nanocomposites (Figure S3, Supporting Information). It can be seen that not only the dispersion state of the CNTs but also the connectivity among the CNTs determined the electrical conductivity of the epoxy nanocomposites. In the epoxy/CNT sponge nanocomposite, the preformed 3D framework ensures the uniform dispersion of the nanotubes and their excellent connection with each other, forming an efficient conducting pathways for electron transport in the epoxy matrix. However, in the epoxy/CNT nanocomposite, most of the CNTs agglomerate together or are isolated without interconnection, causing CNT-rich and CNT-deficient zones. The absence of a continuous percolating CNT network results in a lower electrical conductivity. Moreover, the length of the nanotubes is also a factor affecting the formation of a conducting network and thus the electrical conductivity of the nanocomposites. The exposed parts of the nanotubes on the fracture surface of the epoxy/CNT sponge are notably longer than those of the epoxy/CNT nanocomposite (Figure 1c,d and Figure S4, Supporting Information), suggesting that the longer nanotubes in the sponge facilitate the formation of a conducting network for electron transport, EMI shielding, and load transfer.

Inspired by this remarkable electrical conductivity,[23] we measured the EMI-shielding properties of the epoxy/CNT sponge nanocomposites in the frequency range of 8–12 GHz and compared them with those of epoxy/CNT nanocomposites (**Figure 3**). Neat epoxy and its nanocomposite with 0.66 wt% of CNTs were nearly transparent to electromagnetic waves and their SE values were lower than 2 dB. With increasing CNT content, the EMI SE values of the epoxy nanocomposites present a similar change as that of the electrical conductivity of the same nanocomposites, implying that the EMI SE can be mainly attributed to the formed conducting network

Table 1. Comparison of EMI shielding performance of polymer nanocomposites.

Nanocomposites[a)]	Content	Thickness [mm]	EMI SE [dB]	Frequency	Conductivity [S m^{-1}]	Ref.
Epoxy/carbon black	30 wt%	1	44	1–10 GHz		[2a]
PS/CNF foam	15 wt%		≈19	8.2–12.4 GHz	≈0.1	[13]
PP/MWNT	7.5 vol%	1	34.8	8–12 GHz		[12]
PS/MWNT foam	7 wt%		20	8.2–12.4 GHz		[3b]
PU/SWNT	20 wt%	2	≈17	8.2–12.4 GHz	0.022	[14]
PMMA/SWNT	20 wt%	4.5	30	200–2000 MHz	2	[4b]
			40	8–12 GHz		
Epoxy/Long SWNT	15 wt%	2	23–28	8.2–12.4 GHz	0.2	[15]
RET/SWNT	4.5 vol%	2	≈30	8.2–12.4 GHz		[16]
PCL/MWNT foam	0.25 vol%	20	60–80	25–40 GHz	3.7–4.9	[17]
PMMA/MWNT	40 wt%	0.165	≈27	50 MHz–13.5 GHz		[18]
Epoxy/SWNT	15 wt%	1.5	15–20	500 MHz–1.5 GHz	20	[4a]
Epoxy/RGO	15 wt%		21	8.2–12.4 GHz	≈5	[3i]
PMMA/TGO foam	1.8 vol%	≈2.4	13–19	8–12 GHz	3.11	[19]
PMMA/TGO	4.23 vol%	3.4	≈30	8–12 GHz	20	[1i]
PU/Modified RGO	5 vol%		38	8.2–12.4 GHz	43.64	[20]
PS/RGO	3.47 vol%	2.5	45.1	8.2–12.4 GHz	43.5	[5]
PS/graphene/Fe_3O_4	5 wt%TGO + 8 wt%Fe_3O_4	4	≈30	8–12 GHz	21	[1h]
PDMS/graphene foam	≈0.8 wt%	≈1	≈30	30 MHz–1.5 GHz	200	[7]
			≈20	8–12 GHz		
Epoxy/aligned RGO	2 wt%	>0.1	38	400–4000 MHz	≈1	[3j]
Epoxy/CNT sponge	0.66 wt%	1	25	8–12 GHz	148	This work
	0.66 wt%	2	33		516	This work
	2.0 wt%	2	40			This work

[a)]PP-polypropylene; PU-polyurethane; PMMA-polymethylmethacrylate; PCL-polycaprolactone; PVA-poly(vinyl alcohol); RET-reactive ethylene terpolymer; CNF-carbon nanofiber.

in the epoxy matrix. Note that the EMI SE slightly fluctuates with the frequency. With 10 and 20 wt% of CNTs, the average values of the EMI SE increase to 14 and 24 dB, respectively, which are in accordance with reported values for polymer/CNT nanocomposites.[2b,3c,3d,3f,4a] Interestingly, an extraordinary EMI SE of around 25 dB was achieved for the epoxy/CNT sponge nanocomposite at a low loading of 0.66 wt%, which would be sufficient for commercial applications as EMI-shielding material.[23]

It is well known that the EMI SE is not only dependent on the intrinsic electrical conductivity, the aspect ratio, and dispersion quality of the fillers, but also on the volume and thickness of the polymer specimens. By increasing the specimen thickness from 1 to 2 mm, the average SE value of the epoxy/CNT sponge nanocomposite could be increased from 25 to 33 dB (Figure 3b and Figure S5, Supporting Information). On the other hand only a moderate increase from 24 to 29 dB was observed for the epoxy nanocomposites with 20 wt% of conventional CNTs with the same increase in thickness of the polymer layer.[12] Similar results were observed for the epoxy nanocomposites with different CNT loadings (Figure S6, Supporting Information). Moreover, the EMI SE could also be improved by increasing the filler loading. As shown in Figure 3c, the 2 mm-thick epoxy nanocomposite with 0.66 wt% of CNT sponge exhibited a higher mean value of EMI SE (33 dB) than its counterpart with 0.42 wt% CNT sponge (24 dB). Further increasing the sponge content to 2.0 wt% resulted in a larger mean SE value of 40 dB over the X-band frequency range and a maximum SE of 44 dB was obtained at 8.8 GHz. The far superior EMI-shielding performance of the epoxy/CNT sponge nanocomposite over that of the epoxy/CNT nanocomposite could also be attributed to the preformed 3D CNT framework and the resulting excellent electrical conductivity. The highly conductive CNT network provides abundant interfaces that multiply the reflection and greatly attenuate the incident EM waves inside the nanocomposites. On the other hand, the epoxy/CNT nanocomposites have numerous CNT-deficient zones, are nearly transparent to incident microwaves, and own a low electrical conductivity, which all cause their poor EMI-shielding performance.

To identify the shielding mechanisms of the epoxy nanocomposites, the total EMI SE (SE_{Total}) and the contribution from absorption (SE_A) and reflection (SE_R) at around 8.8 GHz were compared in terms of filler loadings (Figure 3d). The increase in loading resulted in a noticeably improved SE_{Total} and SE_A for

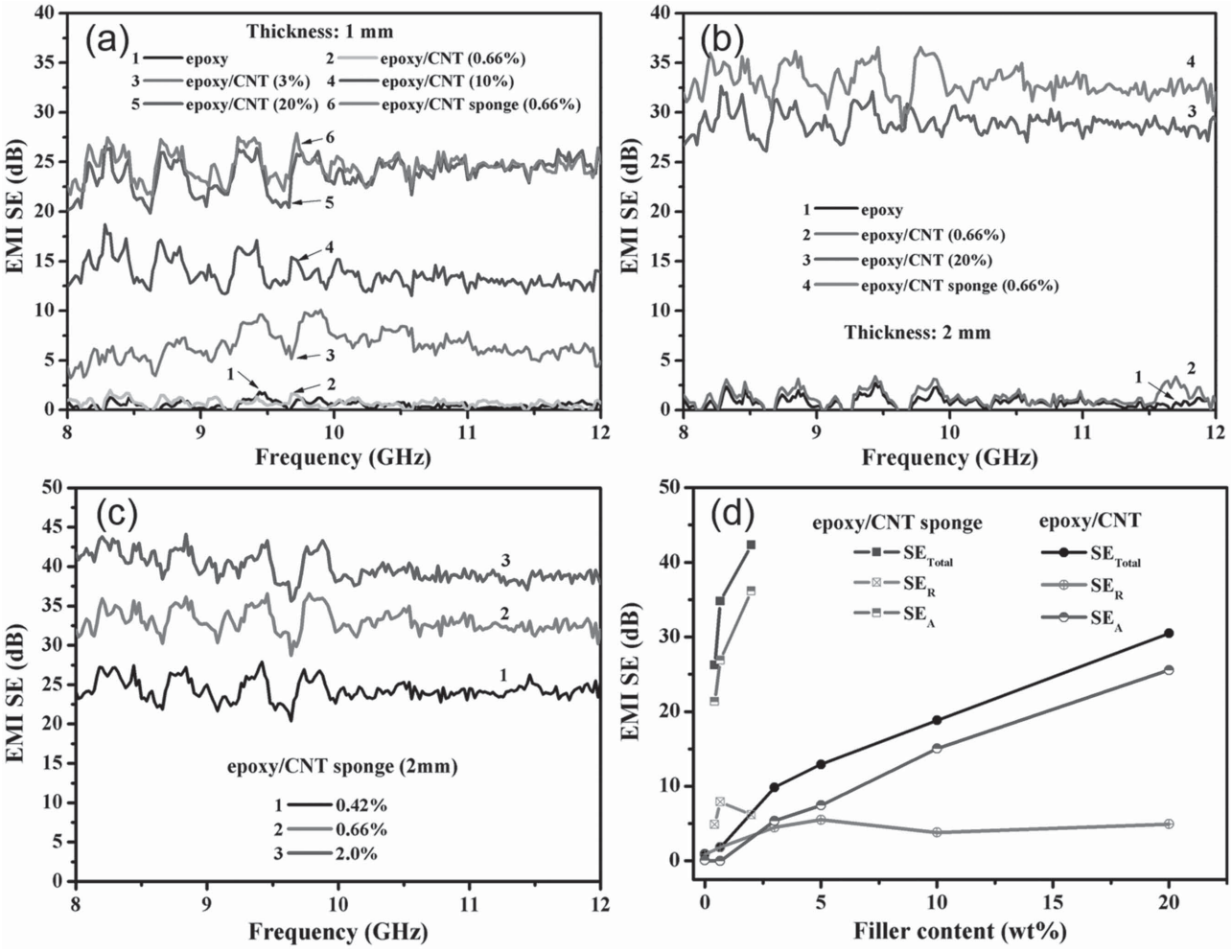

Figure 3. a,b) Plots of EMI SE versus frequency for epoxy nanocomposites filled with CNT sponge and CNTs with specimen thicknesses of: a) 1 mm and b) 2 mm; c) Influence of CNT sponge content on EMI SE in the range of 8–12 GHz; d) Comparison of SE_A and SE_R of epoxy/CNT sponge nanocomposites with those of epoxy/CNT nanocomposites with a specimen thickness of 2 mm.

the epoxy/CNT sponge nanocomposites, whereas the changes in SE_R were less significant. For the nanocomposite with 2.0 wt% CNT sponge, its mean values of SE_{Total}, SE_A and SE_R were 44, 38, and 5 dB, respectively. The increase in SE_A can be attributed to the enhanced connectivity between the nanotubes and thereby the improved electrical conductivity with an increase in filler content. Note that the slight decrease in SE_R observed for the epoxy/CNT sponge with a content higher than 0.66 wt% and for the epoxy/CNT composite with a content higher than 5 wt% can be due to the blocking effect of the conductive CNT network on the reflection of the electromagnetic waves out of the nanocomposites by providing more surfaces to reflect and attenuate the waves inside the nanocomposites.[12] The contribution of the absorption to the attenuation of the electromagnetic radiation was much larger than that of the reflection, indicating an absorption-dominant shielding mechanism of the epoxy/CNT sponge nanocomposites.[1i,7,19]

Table 1 compares the EMI SE and electrical conductivity properties of our epoxy/CNT sponge nanocomposites with those of polymer nanocomposites filled with carbon fillers that have been reported in the literature. Clearly, high loadings of carbon fillers have usually been reported to obtain rather moderate SE values, i.e., 15–20 dB with 15 wt% SWNTs,[4a] 21 dB with 15 wt% RGO,[3i] 30 dB with 4.23 vol% TGO,[1i] or 20 wt% MWNTs.[4b] Li et al.[5] reported a high SE of 45.1 dB at 12.4 GHz with 3.47 vol% RGO and a specimen thickness of 2.5 mm. Kim et al.[3j] reported an SE of 38 dB within the 0.4–4 GHz range for an epoxy nanocomposite filled with 2 wt% highly aligned graphene. Interestingly, PDMS/graphene foam composites have exhibited the highest EMI-shielding performance at low loadings, i.e., around 20 dB for a 1 mm-thick composite and <28 dB for a 2 mm-thick composite at a loading of 0.8 wt%.[7] Our epoxy/CNT sponge nanocomposite, however, presents even higher SE values of 25 dB (1 mm thick) and 33 dB (2 mm thick) at a low sponge content of 0.66 wt%. Therefore, our epoxy/CNT sponge nanocomposite exhibits one of the best shielding performances at low filler loadings,[1f,1i,3e,3j,5,7] indicating its potential as a high-performance EMI shielding material.

In addition to its excellent electrical and EMI-shielding properties, the CNT sponge also provides a remarkable reinforcement to the epoxy nanocomposite, which is necessary for shielding materials that are used in areas where

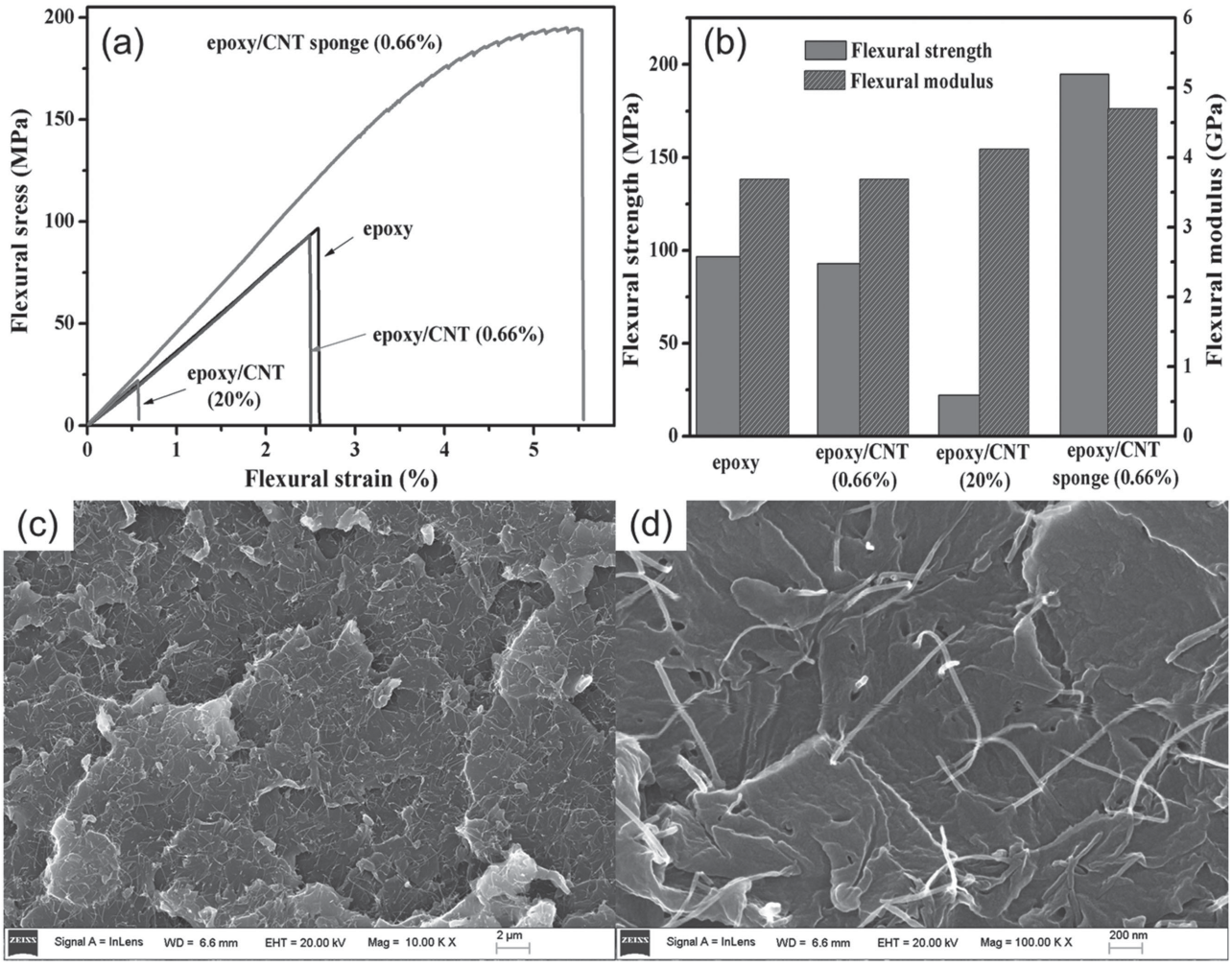

Figure 4. a,b) Flexural properties of neat epoxy and its nanocomposites filled with CNT sponge and CNTs; c,d) SEM images of the fracture surfaces of the epoxy/CNT sponge nanocomposite after flexural testing.

mechanical properties are important. **Figure 4**a,b compares the flexural properties of epoxy nanocomposites filled with either the CNT sponge or separated CNTs. The inclusion of only 0.66 wt% of CNT sponge dramatically enhanced both the flexural strength and modulus by 102% and 27%, respectively, compared to that of neat epoxy. Whereas, the addition of 0.66 wt% separated CNTs did not show any obvious reinforcement as opposed to that of the neat epoxy, indicated by the nearly unchanged flexural properties. For the epoxy nanocomposite with 20 wt% CNTs, its flexural strength was even seriously decreased by 77% due to the embrittlement effect of the CNTs, although its flexural modulus exhibited a moderate increase (12%). Therefore, for a similar EMI-shielding performance, the epoxy/CNT sponge nanocomposite exhibited a flexural strength that was 782% higher than that of its counterpart filled with CNTs.

The prominent reinforcement of the CNT sponge was further confirmed by the tensile performance of its epoxy nanocomposites (Figure S7 and Table S1 in the Supporting Information). Compared to the neat epoxy, the epoxy/CNT sponge nanocomposite exhibited 64% and 97% increases in tensile strength and elongation at break, respectively. However, adding 20 wt% of separated CNTs in the epoxy caused 82% and 88% decreases in tensile strength and elongation at break, respectively. Apart from the significant increase in elongation at break, the tensile toughness (the energy to fracture per unit volume), calculated by integrating the area under the stress–strain curve, can also be employed to compare the toughening effect of different fillers. As expected, the 0.66 wt% CNT sponge again provided a 250% increase in tensile toughness in comparison to that of neat epoxy; whereas 20 wt% of separated CNTs in the epoxy dramatically reduced the tensile toughness by 98%. Furthermore, the incorporation of 0.66 wt% separated CNTs in the epoxy did not bring about any obvious increase in toughness although some positive results have been reported for nanocomposites filled with CNTs and graphene.[6a,6b,33] The CNT sponge structure is therefore far superior to separated CNTs in fabricating strong and tough functional polymer nanocomposites.

To identify the effective reinforcement, the flexural properties were compared with the results obtained for epoxy nanocomposites with CNTs and graphene. It is well known that

Table 2. Enhancement in mechanical properties of epoxy nanocomposites.

Fillers	Content [wt%]	Flexural strength	Flexural modulus	Tensile strength	Young's modulus	Ref.
SWNTs	0.05	10%	17%			[24]
MWNTs	0.3	28%	11.7%			[6c]
	0.4					
MWNTs	6			–25%	32%	[25]
Si-MWNTs	0.2	23.3%	22.4%			[26]
DWNT-NH_2	0.5			8.6%	14.6%	[27]
MWNT-COOH	1	25.5%	54.8%			[28]
FWNT/epoxy film				52.1%	45.8%	[29]
GNPs	1		9%			[30]
GO	0.1	23%	12%		≈12%	[6d]
Modified graphene	0.1	22%	18%			[31]
RGO	0.1			≈40%	≈31%	[6a]
RGO	0.125			≈45%	≈50%	[6b]
Anisotropic qraphene aerogel (||)	1.4	2%	16%			[21]
Graphene foam	0.2	43.7%	57.3%	120.9%		[32]
CVD graphene foam	0.1	38%	53%			[8]
CNT sponge	0.66	102%	27%	64%		This work

nanofillers often provide reinforcement to polymers at low loa dings,[6a,6b,8] and with increasing loading content, the strength and ductility of the nanocomposites tend to decrease. For epoxy nanocomposites, obvious increments of 28% and 23% in the flexural strength were obtained by adding 0.3 wt% pristine MWNTs or 0.1 wt% modified graphene, respectively.[6c,6d] Using a preformed 3D graphene framework, a higher increment of 38% in the flexural strength was achieved as opposed to that in neat epoxy.[8] As far as our CNT sponge was concerned, a much better reinforcement was observed compared to that of the CNTs or graphene, evidenced by the significant 102% increase in flexural strength and 64% increase in tensile strength, which are among the highest values reported for epoxy nanocomposites.[8,21,32] Together with the greatly increased elongation at break and tensile toughness these results confirm the high efficiency of the CNT sponge in toughening the neat epoxy. As a result, a small amount of CNT sponge significantly improved both the strength and toughness of the epoxy, which is quite a challenging achievement because strength and toughness are usually mutually exclusive as the increase in one property often results in sacrificing the other. Similar results have only been observed previously for epoxy nanocomposites with 3D graphene foam.[8] In addition, the relatively moderate increase in flexural modulus may be correlated to the fact that the modulus of a nanocomposite mainly relies on the modulus and volume fraction of its components. Note that most epoxy nanocomposites with excellent mechanical properties listed in **Table 2** are electrically insulating due to the low filler loadings; whereas, our CNT sponge nanocomposite exhibited an extraordinary electrical conductivity and EMI-shielding performance.

To study the reinforcing and toughening mechanisms of the CNT sponge, we examined the fracture-surface morphologies of the neat epoxy and its nanocomposite (Figure 4c,d, and Figure S4, Supporting Information). The neat epoxy had a smooth and featureless fracture surface, which is typical for brittle epoxy (Figure S4a). The addition of 0.66 wt% CNTs caused a similar brittle fracture surface only with slightly increased roughness. The clear interfaces between the CNTs and the matrix, as well as the voids left by pulling out the CNTs indicate the weak interfacial bonding (Figure S4c). When the CNT content was increased to 20 wt%, the fracture surface of the epoxy nanocomposite showed more agglomerates of CNTs and voids, which is consistent with its poor mechanical properties. In contrast, the epoxy/CNT sponge nanocomposite exhibited a rather rugged and rough fracture surface that was densely covered with individual nanotubes. The rougher fracture surface provided a larger surface area for fracture energy absorption.[6b,34] Several pores left by the pulled-out nanotubes suggested a moderate interfacial adhesion between the CNT sponge and the matrix. The visible parts of the CNT sponge show a remarkably longer length (on the order of micrometers) as compared to the separated CNTs observed in epoxy/CNT nanocomposites. Some shorter nanotubes were also observed but these may result from the early breakage of nanotubes under the external load. As has been reported before,[5,34,35] both the pulling out and bridging across crack tips contributed to an enhanced tensile toughness of CNT sponge nanocomposites. The distinct fracture surfaces of the epoxy/CNT and epoxy/CNT sponge nanocomposites may originate from the different filler distributions as illustrated in Figure S3 (Supporting Information). The aggregation of CNTs in the epoxy matrix dramatically reduced the filler–matrix interfaces and initialized cracks under external loading, which deteriorated the mechanical properties of the epoxy nanocomposites. Whereas for the epoxy/CNT sponge nanocomposites, the preformed strong and robust 3D CNT framework throughout the epoxy matrix ensured a uniform dispersion of the nanotubes,

thereby providing a large contact area with the polymer chains, which greatly increased the energy required to pull out the numerous long nanotubes. Furthermore, the interconnected 3D framework can improve the mechanical properties of the epoxy by isotropic and effective stress transfer. Additionally, the much longer nanotubes in the sponge provided better reinforcement to the epoxy than short and separated CNTs. Therefore, the excellent electrical, EMI-shielding, and mechanical properties of epoxy/CNT sponge nanocomposites can be attributed to the more continuous and stronger conductive network for electron transport, EMI shielding, and load transfer.

3. Conclusion

Lightweight and high-performance EMI-shielding epoxy nanocomposites were prepared by impregnating epoxy into a preformed, highly porous, 3D CNT sponge. The highly conductive framework resolved the dispersion problem of separated CNT nanofillers and acted as an efficient bunch of channels for electron transport and struts to resist external loading after compounding with the epoxy. A remarkable electrical conductivity of 148 S m^{-1} and a high EMI SE of around 33 dB in the X-band were achieved for the epoxy nanocomposite with only 0.66 wt% of CNT sponge, which was much higher than that of an epoxy nanocomposite with 20 wt% separated CNTs. More importantly, the CNT sponge also provided the epoxy with the dual advantage of better reinforcement and toughening. Only 0.66 wt% of CNT sponge significantly improved the flexural and tensile strengths by 102% and 64%, respectively, as compared to those of neat epoxy. Moreover, the nanocomposite exhibited a 250% increase in tensile toughness and 97% increase in elongation at break. The outstanding mechanical properties could be attributed to the uniformly dispersed long nanotubes that provide a large interfacial area, and to the interconnected isotropic 3D framework that effectively transfers the external stress. Therefore, by using a 3D CNT sponge, the challenging problem of how to prepare high-performance EMI-shielding materials with excellent mechanical properties can be solved, and this indicates the potential of CNT sponges as ideal candidates for EMI-shielding polymer nanocomposites.

4. Experimental Section

Materials: Epoxy resin, its curing agent (methyl hexahydrophthalic anhydride), and the accelerant (tris(dimethyl aminomethyl) phenol) were all provided by the Jiafa chemical company and Sinopharm Chemical Reagent (China). The CNT sponge was synthesized by CVD using 1,2-dichlorobenzene as the carbon source and ferrocene as the catalyst, as has been reported elsewhere.[10f,11] The diameter and length of the CNTs (porosity >99%) in the sponge were 30–50 nm and 10–50 μm, respectively (Figure S1, Supporting Information). The density of the CNT sponge could be tuned by adjusting the feeding rate of the source and CNT sponges with densities of 5–25 mg cm^{-3} were prepared. For comparison, CNTs with similar diameters (30–50 nm) were bought from Chengdu Organic Chemicals (China) and their lengths were in the range of 10–20 μm.

Preparation of Epoxy Nanocomposites: Epoxy/CNT sponge nanocomposites were prepared using a vacuum-assisted impregnation method. Typically, the epoxy resin, curing agent, and the accelerant were first mixed by a planetary centrifugal vacuum mixer and then impregnated into the highly porous CNT sponge under vacuum. The resulting composite was cured at 80 °C for 4 h followed by 120 °C for 2 h in a vacuum oven and then cut into required shapes for performance measurements. Note that this solvent-free infiltration process avoids the formation of pores derived from solvent evaporation. To fabricate the epoxy/CNT nanocomposites, the separated CNTs were mixed with the epoxy monomer and other additives in the planetary centrifugal vacuum mixer and the mixture was then poured into a mold followed by curing under the same conditions. Specimens with the required shape were thus obtained and polished for relevant measurements.

Characterization: The morphologies of the CNTs and the CNT sponge, as well as their epoxy nanocomposites were observed using a Zeiss Supra55 field-emission SEM and a JEOL 2010 TEM. The electrical conductivities of the neat epoxy and its nanocomposites were measured using a ZC-90G resistivity meter and 4-probes Tech RST-8 resistivity meter. The EMI SE was characterized with a WILTRON 54169A scalar measurement system in the frequency range of 8–12 GHz. The flexural and tensile properties were measured on an electronic universal testing machine at crosshead speeds of 5 and 10 mm min^{-1}, respectively. Specimens of 50 mm × 10 mm × 2 mm were used for flexural and tensile testing and at least five specimens were measured and their average values are reported.

Supporting Information

Supporting Information is available from the Wiley Online Library or from the author.

Acknowledgements

Financial support from the National Natural Science Foundation of China (51373011, 51125010, 51533001), the Fundamental Research Funds for the Central Universities (YS201402), the State Key Laboratory of Organic-Inorganic Composites (201501007) and the China Scholarship Council for Young Scholar Studies Abroad (201406885081) is gratefully acknowledged.

Received: September 7, 2015
Revised: October 9, 2015
Published online: December 9, 2015

[1] a) L. Zhang, N. T. Alvarez, M. Zhang, M. Haase, R. Malik, D. Mast, V. Shanov, *Carbon* **2015**, *82*, 353; b) W. L. Song, L. Z. Fan, M. S. Cao, M. M. Lu, C. Y. Wang, J. Wang, T. T. Chen, Y. Li, Z. L. Hou, J. Liu, Y. P. Sun, *J. Mater. Chem. C* **2014**, *2*, 5057; c) W. L. Song, M. S. Cao, M. M. Lu, S. Bi, C. Y. Wang, J. Liu, J. Yuan, L. Z. Fan, *Carbon* **2014**, *66*, 67; d) K. Ji, H. Zhao, Z. Huang, Z. Dai, *Mater. Lett.* **2014**, *122*, 244; e) B. Shen, W. Zhai, W. Zheng, *Adv. Funct. Mater.* **2014**, *24*, 4542; f) S. T. Hsiao, C. C. Ma, W. H. Liao, Y. S. Wang, S. M. Li, Y. C. Huang, R. B. Yang, W. F. Liang, *ACS Appl. Mater. Interfaces* **2014**, *6*, 10667; g) W. L. Song, J. Wang, L. Z. Fan, Y. Li, C. Y. Wang, M. S. Cao, *ACS Appl. Mater. Interfaces* **2014**, *6*, 10516; h) Y. Chen, Y. Wang, H. B. Zhang, X. Li, C. X. Gui, Z. Z. Yu, *Carbon* **2015**, *82*, 67; i) H. B. Zhang, W. G. Zheng, Q. Yan, Z. G. Jiang, Z. Z. Yu, *Carbon* **2012**, *50*, 5117.

[2] a) N. A. Aal, F. El-Tantawy, A. Al-Hajry, M. Bououdina, *Polym. Compos.* **2008**, *29*, 125; b) A. Ameli, P. U. Jung, C. B. Park, *Carbon* **2013**, *60*, 379.

[3] a) S. Pande, A. Chaudhary, D. Patel, B. P. Singh, R. B. Mathur, *RSC Adv.* **2014**, *4*, 13839; b) Y. L. Yang, M. C. Gupta, *Nano Lett.* **2005**, *5*, 2131; c) A. Gupta, V. Choudhary, *J. Mater. Sci.* **2011**, *46*, 6416; d) V. K. Sachdev, S. Bhattacharya, K. Patel, S. K. Sharma, N. C. Mehra, R. P. Tandon, *J. Appl. Polym. Sci.* **2014**, *131*, 40201; e) S. Maiti, N. K. Shrivastava, S. Suin, B. B. Khatua, *ACS Appl. Mater. Interfaces* **2013**, *5*, 4712; f) D. X. Yan, P. G. Ren, H. Pang,

Q. Fu, M. B. Yang, Z. M. Li, *J. Mater. Chem.* **2012**, *22*, 18772; g) B. Wen, M. Cao, M. Lu, W. Cao, H. Shi, J. Liu, X. Wang, H. Jin, X. Fang, W. Wang, J. Yuan, *Adv. Mater.* **2014**, *26*, 3484; h) T. K. Gupta, B. P. Singh, V. N. Singh, S. Teotia, A. P. Singh, I. Elizabeth, S. R. Dhakate, S. K. Dhawan, R. B. Mathur, *J. Mater. Chem. A* **2014**, *2*, 4256; i) J. Liang, Y. Wang, Y. Huang, Y. Ma, Z. Liu, F. Cai, C. Zhang, H. Gao, Y. Chen, *Carbon* **2009**, *47*, 922; j) N. Yousefi, X. Sun, X. Lin, X. Shen, J. Jia, B. Zhang, B. Tang, M. Chan, J. K. Kim, *Adv. Mater.* **2014**, *26*, 5480.

[4] a) N. Li, Y. Huang, F. Du, X. B. He, X. Lin, H. J. Gao, Y. F. Ma, F. F. Li, Y. S. Chen, P. C. Eklund, *Nano Lett.* **2006**, *6*, 1141; b) N. C. Das, Y. Liu, K. Yang, W. Peng, S. Maiti, H. Wang, *Polym. Eng. Sci.* **2009**, *49*, 1627.

[5] D. X. Yan, H. Pang, B. Li, R. Vajtai, L. Xu, P. G. Ren, J. H. Wang, Z. M. Li, *Adv. Funct. Mater.* **2015**, *25*, 559.

[6] a) M. A. Rafiee, J. Rafiee, Z. Wang, H. Song, Z. Z. Yu, N. Koratkar, *ACS Nano* **2009**, *3*, 3884; b) M. A. Rafiee, J. Rafiee, I. Srivastava, Z. Wang, H. Song, Z. Z. Yu, N. Koratkar, *Small* **2010**, *6*, 179; c) Y. Zhou, F. Pervin, L. Lewis, S. Jeelani, *Mater. Sci. Eng. A* **2008**, *475*, 157; d) D. R. Bortz, E. Garcia Heras, I. Martin-Gullon, *Macromolecules* **2012**, *45*, 238.

[7] Z. Chen, C. Xu, C. Ma, W. Ren, H. M. Cheng, *Adv. Mater.* **2013**, *25*, 1296.

[8] J. Jia, X. Sun, X. Lin, X. Shen, Y. W. Mai, J. K. Kim, *ACS Nano* **2014**, *8*, 5774.

[9] Z. Chen, W. Ren, L. Gao, B. Liu, S. Pei, H. M. Cheng, *Nat. Mater.* **2011**, *10*, 424.

[10] a) H. Li, X. Gui, L. Zhang, S. Wang, C. Ji, J. Wei, K. Wang, H. Zhu, D. Wu, A. Cao, *Chem. Commun.* **2010**, *46*, 7966; b) W. Zhao, Y. Li, S. Wang, X. He, Y. Shang, Q. Peng, C. Wang, S. Du, X. Gui, Y. Yang, Q. Yuan, E. Shi, S. Wu, W. Xu, A. Cao, *Carbon* **2014**, *76*, 19; c) J. Zhong, Z. Yang, R. Mukherjee, A. Varghese Thomas, K. Zhu, P. Sun, J. Lian, H. Zhu, N. Koratkar, *Nano Energy* **2013**, *2*, 1025; d) X. Chen, H. Zhu, Y. C. Chen, Y. Shang, A. Cao, L. Hu, G. W. Rubloff, *ACS Nano* **2012**, *6*, 7948; e) M. Crespo, M. González, A. L. Elías, L. Pulickal Rajukumar, J. Baselga, M. Terrones, J. Pozuelo, *Phys. Status Solidi RRL* **2014**, *8*, 698; f) X. Gui, H. Li, L. Zhang, Y. Jia, L. Liu, Z. Li, J. Wei, K. Wang, H. Zhu, Z. Tang, D. Wu, A. Cao, *ACS Nano* **2011**, *5*, 4276.

[11] X. Gui, J. Wei, K. Wang, A. Cao, H. Zhu, Y. Jia, Q. Shu, D. Wu, *Adv. Mater.* **2010**, *22*, 617.

[12] M. H. Al-Saleh, U. Sundararaj, *Carbon* **2009**, *47*, 1738.

[13] Y. L. Yang, M. C. Gupta, K. L. Dudley, R. W. Lawrence, *Adv. Mater.* **2005**, *17*, 1999.

[14] Z. Liu, G. Bai, Y. Huang, Y. Ma, F. Du, F. Li, T. Guo, Y. Chen, *Carbon* **2007**, *45*, 821.

[15] Y. Huang, N. Li, Y. Ma, D. Feng, F. Li, X. He, X. Lin, H. Gao, Y. Chen, *Carbon* **2007**, *45*, 1614.

[16] S. H. Park, P. Thielemann, P. Asbeck, P. R. Bandaru, *Appl. Phys. Lett.* **2009**, *94*, 243111.

[17] J. M. Thomassin, C. Pagnoulle, L. Bednarz, I. Huynen, R. Jerome, C. Detrembleur, *J. Mater. Chem.* **2008**, *18*, 792.

[18] H. M. Kim, K. Kim, C. Y. Lee, J. Joo, S. J. Cho, H. S. Yoon, D. A. Pejakovic, J. W. Yoo, A. J. Epstein, *Appl. Phys. Lett.* **2004**, *84*, 589.

[19] H. B. Zhang, Q. Yan, W. G. Zheng, Z. He, Z. Z. Yu, *ACS Appl. Mater. Interfaces* **2011**, *3*, 918.

[20] S. T. Hsiao, C. C. M. Ma, H. W. Tien, W. H. Liao, Y. S. Wang, S. M. Li, C. Y. Yang, S. C. Lin, R. B. Yang, *ACS Appl. Mater. Interfaces* **2015**, *7*, 2817.

[21] Z. Wang, X. Shen, M. A. Garakani, X. Lin, Y. Wu, X. Liu, X. Sun, J. K. Kim, *ACS Appl. Mater. Interfaces* **2015**, *7*, 5538.

[22] H. B. Zhang, W. G. Zheng, Q. Yan, Y. Yang, J. W. Wang, Z. H. Lu, G. Y. Ji, Z. Z. Yu, *Polymer* **2010**, *51*, 1191.

[23] D. D. L. Chung, *Carbon* **2001**, *39*, 279.

[24] M. Moniruzzaman, F. M. Du, N. Romero, K. I. Winey, *Polymer* **2006**, *47*, 293.

[25] Y. Breton, G. Desarmot, J. P. Salvetat, S. Delpeux, C. Sinturel, F. Beguin, S. Bonnamy, *Carbon* **2004**, *42*, 1027.

[26] J. Kathi, K. Y. Rhee, J. H. Lee, *Compos. Part A, Appl. Sci. Manuf.* **2009**, *40*, 800.

[27] F. H. Gojny, M. H. G. Wichmann, B. Fiedler, K. Schulte, *Compos. Sci. Technol.* **2005**, *65*, 2300.

[28] M. Theodore, M. Hosur, J. Thomas, S. Jeelani, *Mater. Sci. Eng. A* **2011**, *528*, 1192.

[29] Y. Hou, J. Tang, H. Zhang, C. Qian, Y. Feng, J. Liu, *ACS Nano* **2009**, *3*, 1057.

[30] S. Chatterjee, F. Nafezarefi, N. H. Tai, L. Schlagenhauf, F. A. Nueesch, B. T. T. Chu, *Carbon* **2012**, *50*, 5380.

[31] M. Naebe, J. Wang, A. Amini, H. Khayyam, N. Hameed, L. H. Li, Y. Chen, B. Fox, *Sci. Rep.* **2014**, *4*, 4375.

[32] Y. Ni, L. Chen, K. Teng, J. Shi, X. Qian, Z. Xu, X. Tian, C. Hu, M. Ma, *ACS Appl. Mater. Interfaces* **2015**, *7*, 11583.

[33] F. Yavari, M. A. Rafiee, J. Rafiee, Z. Z. Yu, N. Koratkar, *ACS Appl. Mater. Interfaces* **2010**, *2*, 2738.

[34] M. Kaleemullah, S. U. Khan, J. K. Kim, *Compos. Sci. Technol.* **2012**, *72*, 1968.

[35] B. Wetzel, P. Rosso, F. Haupert, K. Friedrich, *Eng. Fract. Mech.* **2006**, *73*, 2375.